



## NUMERICAL ANALYSIS OF EROSION IN CYCLONES CONSIDERING INTER-PARTICLE COLLISION

### Diego Alves de Moro Martins

Federal Center for Technological Education of Minas Gerais, Campus Araxá  
Av. Min. Olavo Drummond, 25 - Araxá - Minas Gerais - Brazil. ZIP: 38180-510  
e-mail: diegomoro@cefetmg.br

### Francisco José de Souza

School of Mechanical Engineering - Federal University of Uberlândia  
Av. João Naves de Ávila, 2121 Bloco 5P - Uberlândia - Minas Gerais - Brazil, ZIP: 38400-902  
e-mail: francisco.souza@ufu.br

### Ricardo de Vasconcelos Salvo

Federal Technologic University of Parana, Campus Londrina.  
Av. dos Pioneiros, 3131 - Londrina - Parana - Brazil. ZIP: 86036-370  
e-mail: ricardosalvo@utfpr.edu.br

**Abstract.** Cyclones separators are commonly used in industry to separate particles from gases. The collection efficiency in these devices can reach 99%. Despite their high efficiency, the use of cyclones for separating particles may be impractical due to high wear caused by collision of particles with the walls. In this paper, the particle-gas flow in a cyclone separator will be simulated using the Euler/Lagrange approach. The exchange of momentum between particles and fluid, and the collision between particles will be modelled using the four-way coupling method. The effect of collision between particles and particle/wall will be analyzed, and the wear will be estimated using an erosion correlation. Some interesting effects involving the exchange of momentum between the fluid and the particles will be also discussed.

**Keywords:** Cyclone erosion, Four-way coupling, LES, Inter-particle collision, Shielding effect.

## 1. INTRODUCTION

In several engineering applications, a surface is attacked by solid particles carried by a fluid, resulting in an undesired superficial wear to the component or piece of equipment. This kind of abrasive wear is referred to as erosion and occurs frequently in industrial operations. The erosion effects can be observed in the oil and gas industry, more specifically in the transportation and processing sectors. In the Fluid Catalytic Cracking (FCC) unit, catalyst particles are deliberately added to the process for accelerating chemical reactions. These particles are separated and reused in a cyclic process. The separation occurs through cyclone banks present in the reactor and regenerator of FCC units. The mechanical wear caused by the particles in cyclones is the main cause of unscheduled shutdowns in FCC units (Chen, 2013). Currently, it is of great interest for industries and technology centers to obtain reliable tools to predict and solve this issue, with the purpose of saving time, resources and environmental complications due to potential spillage.

The purpose of this work is to analyze the erosion in a cyclone separator similar to a second-stage cyclone of a FCC unit by means of CFD. The Eulerian-Lagrangian formulation was employed to solve the fluid flow and particle motion. The exchange of momentum between particles and fluid, and collision between particles are modelled through the four-way coupling method. The effect of mass loading on the inter-particle and particle/wall collisions is analyzed and the resulting erosion is accounted by an empirical correlation.

Due to the problem complexity, only a few studies on erosion in cyclone separators have been published. Numerical and experimental analyses were made by Danyluk et al. (1980). They made experiments in a stainless-steel cyclone and compare the results with Finnie's model. Karri et al. (2011) made experiments in a cyclone similar to a second-stage cyclone of a FCC unit. The experiments were accomplished in cyclones with multiple coatings of drywall joint compound added to the wall. The amount of erosion occurring in the cyclone was measured by the weight loss of the drywall compound occurring over a certain period. Numerical simulations were made by Utikar et al. (2010) predicting erosion in cyclone separators. The Eulerian-Lagrangian formulation with two-way coupling method was employed. No papers were found about erosion in cyclones, using the four-way coupling method.

Given subject complexity and high cost of the equipment needed to carry out experiments in cyclones with metallic walls required alternative and cheaper materials were used. Most experiments were performed in acrylic or drywall

cyclones. Nevertheless, the empirical correlations to predict the erosion were developed for metallic walls. In this context, it was not possible to perform a quantitative comparison between the numerical results and experimental ones.

The numerical analysis was performed on the same geometry studied by Karri et al. (2011). As mentioned above, the experiments were accomplished in a cyclone with coatings of drywall added to the wall. Due to the difference among the materials employed in the models, the comparison, between the numerical results and experimental ones, was performed in a qualitative way.

## 2. MODELLING

### 2.1 Gas phase model

The filtered Navier-Stokes equations with Smagorinsky turbulence model (Smagorinsky, 1964) was adopted in this investigation. This sub-grid scale model was chosen due to the good accuracy to solve turbulent rotational flows (Souza et al., 2012). The equations based in the Boussinesq hypotheses can be written in tensor notation as:

$$\frac{\partial \bar{\rho} \bar{u}_i}{\partial x_i} = 0, \quad (1)$$

$$\frac{\partial \bar{\rho} \bar{u}_i}{\partial t} + \frac{\partial}{\partial x_j} (\bar{\rho} \bar{u}_i \bar{u}_j) = -\frac{\partial \bar{p}}{\partial x_i} + \frac{\partial}{\partial x_j} \left[ (\mu + \mu_t) \left( \frac{\partial \bar{u}_i}{\partial x_j} + \frac{\partial \bar{u}_j}{\partial x_i} \right) \right] + S_{\bar{u}_i p}. \quad (2)$$

In the equations above,  $\rho$  and  $\mu$  are the fluid density and viscosity, respectively, the overbar denotes the filtered quantity,  $S_{\bar{u}_i p}$  is the source term due to interaction with the dispersed phase,  $\mu_t$  is the eddy viscosity and represents the energy dissipation present in the smallest scales of flow, which are not resolved in LES, and must be modeled:

$$\mu_t = \rho (C_S \Delta^2) \bar{S}, \quad (3)$$

$\Delta$  is the grid filter length,  $\bar{S}$  is the filtered shear strain rate and  $C_S$  is the Van Driest damping function.

The numerical solution of the conservation equations for the momentum and turbulence, is accomplished by the computational code UNSCYFL3D. This in-house tool is based on the finite volume method in unstructured three-dimensional grids. The SIMPLE (Semi-Implicit Method for Pressure-Linked Equations) algorithm is used to couple the velocity and pressure fields.

### 2.2 Particle motion model

As mentioned in the previous section, the dispersed phase was treated in a Lagrangian framework, in which each particle is tracked through the domain and its equation of motion is based on Newton's second law. The trajectory, linear momentum and angular momentum conservation equations for a rigid, spherical particle can be written, respectively, as:

$$\frac{dx_{pi}}{dt} = u_{pi}, \quad (4)$$

$$m_p \frac{du_{pi}}{dt} = m_p \frac{3\rho C_D}{4\rho_p d_p} (u_i - u_{pi}) + F_{s_i} + F_{r_i} + \left( 1 - \frac{\rho}{\rho_p} \right) m_p g_i, \quad (5)$$

$$I_p \frac{d\omega_{pi}}{dt} = T_i. \quad (6)$$

In the above equations,  $u_i$  is the filtered velocity,  $u_{pi}$  and  $\omega_{pi}$  are the linear and angular particle velocity, respectively.  $d_p$  and  $\rho_p$  are the particle diameter and particle density, respectively.  $C_D$  is the drag coefficient,  $F_{s_i}$  is the shear-induced lift force,  $F_{r_i}$  is the rotation-induced lift,  $T_i$  is the particle torque and  $I_p$  is the moment of inertia for a sphere.

The source term in Eq. (2) is due to the momentum transferred by the particles. This momentum is computed via the Particle-Source-in-Cell concept (PSI Cell). Instead of adding all the dynamic forces acting in the particles, the momentum

transferred is evaluated through the temporal variation of the particle speed when they pass through the cell. In this process, external forces should be subtracted, resulting in the following expression for the source term:

$$S_{\bar{u}_i p} = \frac{-1}{V_{cv}} \sum_k m_k N_k \times \frac{1}{\Delta t} \sum_n \left\{ \left( [u_{p,i}]_k^{(n+1)} - [u_{p,i}]_k^n \right) - g_i \left( 1 - \frac{\rho}{\rho_p} \right) \Delta t_L \right\}, \quad (7)$$

$k$  is related to the number of particles that passed through the cell,  $m_k$  is the mass of each particle which pass through the cell and  $N_k$  is the number of real particles that a computational particle represents.  $n$  is related to the sub-time-steps of the particles and  $\Delta t_L$  is the Lagrangian time-step.

Inter-particle collisions are modeled by a stochastic, hard-sphere model. As described by Oesterlé and Petitjean (1993) and Sommerfeld (2001).

### 2.3 Erosion model

Several erosion models were verified by Pereira et al. (2014) to predict, numerically, the erosion in a 90° bend. The model proposed by Oka et al. (2005) showed the most suitable results when compared to experimental ones Chen et al. (2014). Duarte et al. (2015 and 2016) have also verified the reliability of the model. In this context, the erosion model proposed by Oka et al. (2005) was employed to predict the erosion in this work.

The authors put forward that the effective parameters for erosion damage should include impact velocity, angle, size and type of particles and material hardness as one of mechanical properties of a target material. The model was developed for several metallic materials and three types of particles: angular SiO<sub>2</sub>, SiC and glass beads (GB). In this work, the model was adapted for the pair sand–aluminum, as well as the materials of the restitution correlation proposed by Grant e Tabakoff (1975)

According Duarte et al. (2015 and 2016), the equations of Oka et al. (2005) for SiO<sub>2</sub> and aluminum might be adapted as follows:

$$E(\alpha) = g(\alpha) E_{90}. \quad (8)$$

$E(\alpha)$  and  $E_{90}$  denote a unit of eroded material per mass of particles (mm<sup>3</sup>/kg).  $g(\alpha)$  is the impact angle dependence expressed by two trigonometric functions and by the initial eroded material Vickers hardness number ( $H_v$ ) in GPa, as in Eq. (39):

$$g(\alpha) = (\sin \alpha)^{n_1} [1 + H_v (1 - \sin \alpha)]^{n_2}. \quad (9)$$

The reference erosion ratio  $E_{90}$  (erosion damage at normal impact angle) is related to the impact velocity, particle diameter and eroded material hardness, and can be expressed, for the pair sand-aluminum, as follows:

$$E_{90} = 81,714 (H_v)^{-0,79} \left( \frac{V_p}{V_p^*} \right)^{k_2} \left( \frac{D_p}{D_p^*} \right)^{k_3}. \quad (10)$$

$V_p$  and  $D_p$  are the impact velocity and particle diameter, respectively. The model constants for SiO<sub>2</sub> and aluminum are shown in Tab. 1.

Table 1. Constants of the erosion model proposed by Oka et al. [27], considering the pair sand-aluminum.

Reference velocity $V_p^*$	104 m/s
Reference diameter $D_p^*$	326 μm
$n_1$	0.7148
$n_2$	2.2945
$k_2$	2.3042
$k_3$	0.19

To convert  $E(\alpha)$  to erosion ratio  $E_r$  (eroded mass per particle mass), it is necessary to use a conversion factor:

$$E_r = 1,0 \cdot 10^{-9} \rho_w E(\alpha), \quad (11)$$

$\rho_w$  is the wall density. The conversion is performed to the international system of units.

Usually, the erosion wear is analyzed in function of the erosion rate,  $E_t$  (eroded mass per unit of area per unit of time), or the penetration ratio,  $RP$  (thickness of eroded material per particle mass), and can be expressed as follows:

$$E_t = \frac{1}{A_f} \sum_{m(f)} \dot{m}_\pi E_r, \quad (12)$$

$$RP = \frac{E_t}{\dot{m} \rho_w}, \quad (13)$$

here  $A_f$  is the area of the face collided,  $\dot{m}_\pi$  is the particle mass flow rate represented by each computational particle that collides with the face and  $\dot{m}$  is the inlet particle mass flow rate.

### 3. RESULTS

#### 3.1 Model validation

As previously mentioned, it was not possible to achieve a quantitative validation of the erosion model in cyclones. Therefore, the computational model was validated by comparing the numerical results with the experimental ones obtained by Mazumder et al. (2008). Their experiments consisted in a pneumatic conveying of solid particles in an aluminum elbow. The authors verified the thickness loss along the curve.

Figure 1 shows the penetration ratio profile comparing the numerical results with the experimental ones.

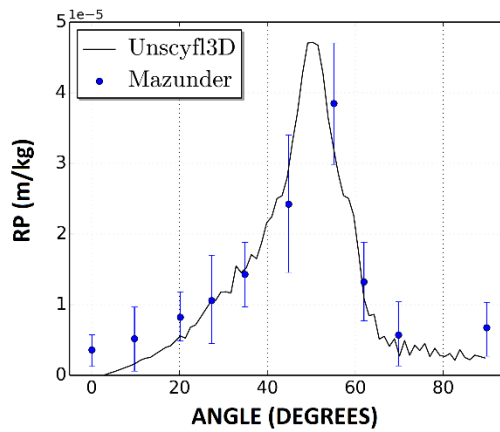


Figure 1. Profile of the penetration ratio along the curve.

#### 3.2 Cyclone erosion

The geometry employed in the simulations to analyze erosion in cyclone was the same used by Karri et al. (2011) in their experiments. Figure 2 shows a schematic of the cyclone with the dimensions.

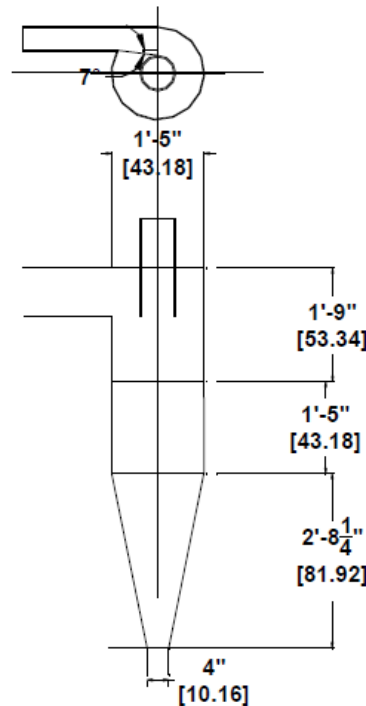


Figure 2. Schematic of the experimental cyclone [mm] (adapted from Karri et al. (2011)).

The parameters employed in the numerical model were the same to those of the experiment made by Karri et al. (2011), except for the wall material. The experiments were made in a cyclone with multiple coatings of drywall joint compound added to the wall and, due to the erosion model, it was used aluminum as wall material in the numerical simulations. Table 2 summarize the simulation parameters.

Table 2. Simulation parameters.

Fluid	Air
Inlet velocity	19;8 m/s
Reynolds	≈540.000
Mass loading	0,00912 kg <sub>p</sub> /kg <sub>g</sub>
Cyclone material	Aluminum (6061-T6)
Cyclone density	2,700 kg/m <sup>3</sup>
Vickers hardness	1.049 GPa
Particle type	SiO <sub>2</sub>
Particle density	1,490 kg/m <sup>3</sup>
Computational mesh	1,800,000 hexahedral volumes

Initially, it was verified the influence of the coupling methods used in this work (one, two and four-way). In the one-way method, the fluid forces influence the particle behavior, but the fluid itself is not influenced by the particles. In the two-way method, there is an exchange of momentum between the phases. In the four-way method, there is an exchange of momentum between the phases and between the particles.

The inter-particle collision modelled by the four-way coupling method causes an increase in particle concentration inside the cyclone. This effect reduces the particle concentration at the wall, especially in regions with higher number of particles. Figures 3, 4 and 5 show the profiles, respectively, of the particle concentration, impact velocity and impact angle along the cylinder and cone of the cyclone, from bottom to top.

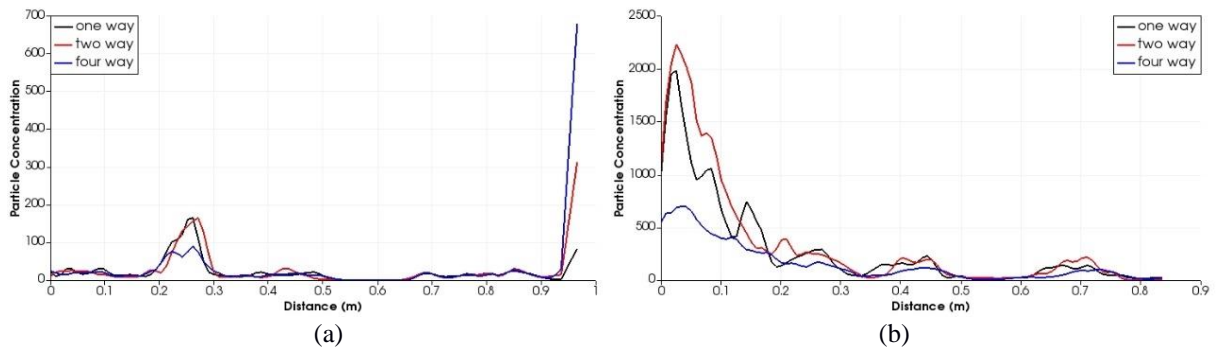


Figure 3. Particle concentration profile along the cylinder (a) and cone (b), from bottom to top.

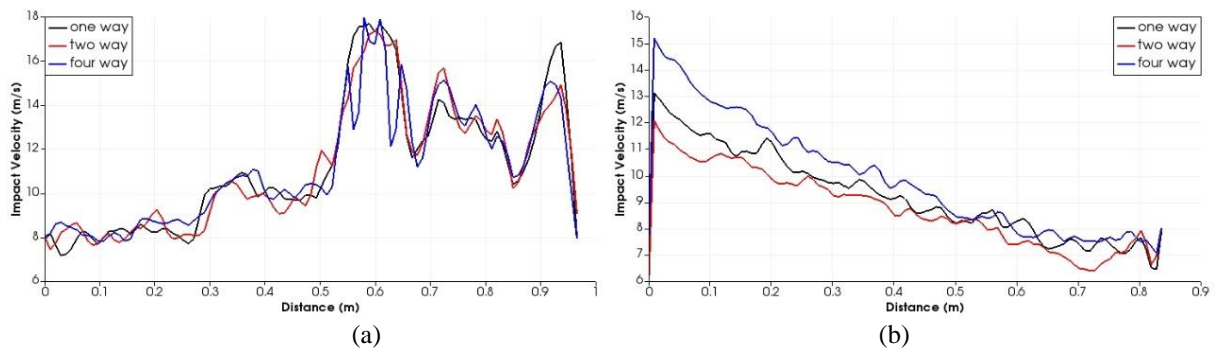


Figure 4. Impact velocity profile along the cylinder (a) and cone (b), from bottom to top.

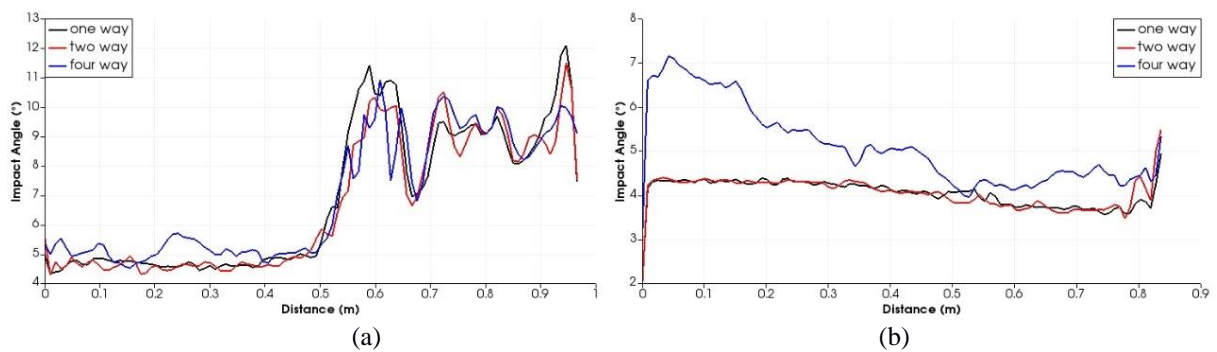


Figure 5. Impact angle profile along the cylinder (a) and cone (b), from-bottom to top.

Figure 6 shows the contour of the penetration ratio for the coupling methods considered in this work and Fig. 7 shows the penetration ratio profile along the cylinder and cone, from bottom to top.

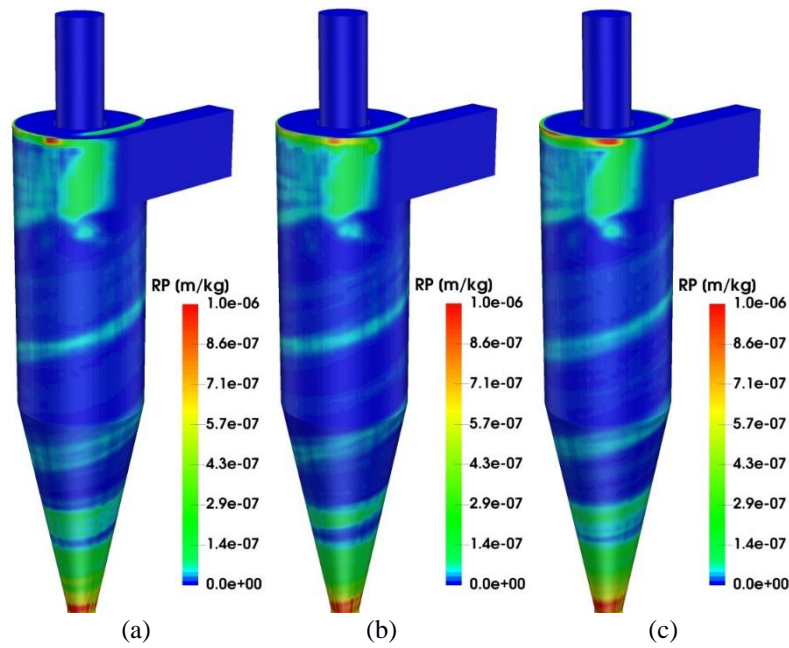


Figure 6. Contour of the impact angle for one-way (a), two-way (b) and four-way (c) coupling methods.

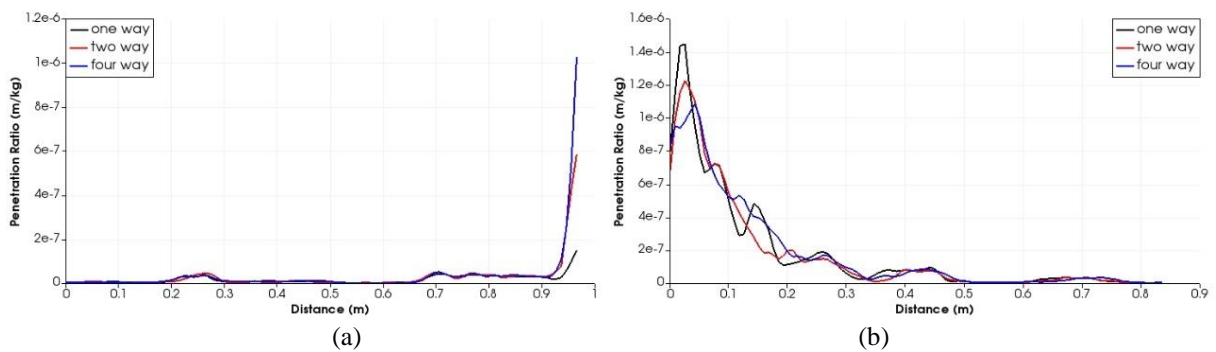


Figure 7. Penetration ratio profile along the cylinder (a) and cone (b), from bottom to top.

It was noted in Figs. 6 and 7 that the penetration ratio changed according to the modelled effects. The difference was observed principally with the four-way coupling method. In this model, the “shielding effect” could be observed in the cone bottom (Fig. 7 (b)). In such region, the penetration ratio was minor when compared with one-way and two-way methods. This effect occurred due to the low particle concentration, as show in Fig. 3 (b). The penetration ratio was more diffused along the wall with the four-way method. This occurred due to the inter-particle collision which caused a scattering of the particles along the wall. The scattering of particles and the relative high velocity and angle of impact (Figs. 4 and 5) caused an increase in the penetration ratio with the four-way coupling method. This effect could be noted in the results of Tab. 3, which showed the erosion rate obtained in the cyclone, comparing the coupling methods and the cyclone parts.

Table 3. Erosion rate obtained through the simulations.

Coupling Methods	Cylinder	Erosion rate (g/h)	
		Cone	Total
One-way	0.2559	0.7039	0.9629
Two-way	0.2686	0.6750	0.9436
Four-way	0.3007	0.8234	1.1241

In the experiments made by Karri et al. (2011), the amount of erosion occurring in the cyclone was measured by the weight loss of the drywall compound occurring over a certain period of time. The authors found that the erosion took place primarily in the bottom 1/3 of the cone of the secondary cyclone, as showed in Fig. 8. Tab. 4 shows the erosion rate obtained experimentally.



Figure 8. Photograph of Erosion of drywall in the cone of a second-stage Cyclone (Karri et al. (2011)).

Table 4. Erosion rate obtained experimentally (Karri et al. (2011)).

Cyclone Region	Erosion rate
Cone	$\approx 680$ g/h
Cylinder	$\approx 105$ g/h

The erosion rate obtained experimentally is much higher than the simulation ones. This difference is due the material properties employed in the simulations, aluminum has a higher abrasion resistance than drywall. However, the region with more erosion are the same, i.e., the cone of the cyclone, showing the predictive ability of the model, leastways qualitatively. To perform a quantitative comparison, it was necessary empirical correlations developed for the same materials used in the experiments.

#### 4. CONCLUSIONS

In this work, numerical simulations to predict erosion in cyclones were accomplished. The numerical model included the gas-solid interaction and inter-particle collision, characterizing a four-way coupling model with the Eulerian-Lagrangian approach. The results were compared to the experiments made by Karri et al. (2011). The erosion regions obtained numerically were the same of the experimental ones. However, due to the simplifications in the model, the magnitude was different. The computational model was adapted to spherical sand particles and aluminum wall, while the experiments were made with angular catalyst particles and wall with drywall joint compound.

Also, a comparison was carried out between the coupling methods (one, two and four-way). The wear obtained with the four-way coupling method was a little higher than that obtained with the other methods. The inter-particle collision, modelled by the four-way coupling method, caused a higher dispersion between the particles. This spreading increased the wall area impacted by the particles, resulting in a bigger wear. Another observation was the shielding effect caused by the particles nearest to the walls, which avoided collision of other particles against the wall.

There was no significant difference between one and two-way coupling methods, probably due the low mass loading employed in the simulations.

#### 5. ACKNOWLEDGEMENTS

The authors thank the National Counsel of Technological and Scientific Development (CNPq) for the financial support.

#### 6. REFERENCES

- Chen, X., McLaury, B.S. and Shirazi, S., 2004. "Application and Experimental Validation of a Computational Fluid Dynamics (CFD) - Based Erosion Prediction Model in Elbows and Plugged Tees", *Computers & Fluids*, Vol. 33.
- Chen, Y., 2013. "Evolution of FCC - Past Present and Future and The Challenges of Operating a High Temperature CFB System", 10th International Conference on Circulating Fluidized Beds and Fluidization Technology, Volume RP7.
- Danyluk, S., Shack, W. J. and Park, J. Y., 1980. "The erosion of a type 310 stainless steel cyclone from a coal gasification pilot plant", *Wear*, Vol. 63.

- Duarte, C.A.R., Souza, F.J. and Santos, V.F., 2015. "Numerical investigation of mass loading effects on elbow erosion", Powder Technol., Vol. 283.
- Duarte, C.A.R., Souza, F.J. and Santos, V.F., 2016. "Mitigating elbow erosion with a vortex chamber", Powder Technol., Vol. 288.
- Grant, G. and Tabakoff, W., 1975. "Erosion prediction in turbomachinery resulting from environmental solid particles", Journal of Aircraft, Vol. 12.
- Karri, R. S. B., Cocco R. and Knowlton, T., 2011. "Erosion in Second Stage Cyclones: Effects of Cyclone Length and Outlet Gas Velocity", 10th International Conference on Circulating Fluidized Beds and Fluidization Technology, Spring.
- Mazumder, Q. H.; Shirazi, S. A. e Mclaury, B., 2008. "Experimental investigation of the location of maximum erosive wear damage in elbows", Journal of Pressure Vessel Technology, Vol. 130.
- Pereira, G.C., Souza, F.J. and Martins D.A.M., 2014. "Numerical prediction of the erosion due to particles in elbows", Powder Technol., Vol. 261.
- Smagorinsky, J., 1963 "General Circulation Experiments with the Primitive Equations", Monthly Weather. Rev. 91.
- Souza, F.J., Vasconcelos Salvo, R. Moro Martins, D.A., 2012. "Large eddy simulation of the gas-particle flow in cyclone separators", Sep. Purif. Technol., Vol. 94.
- Oesterle, B. and Petitjean, A., 1993. "Simulation of particle-to-particle interactions in gas solid flows", Int. J. Multiphase Flow, Vol. 19.
- Sommerfeld, M., 2001. "Validation of a stochastic lagrangian modelling approach for interparticle collisions in homogeneous isotropic turbulence", Int. J. Multiphase Flow, Vol. 27.
- Oka, Y., Okamura, K. and Yoshida, T., 2005. "Practical estimation of erosion damage caused by solid particle impact", Wear, Vol. 259.
- Utikar, R., Darmawan, N. Tade, M., Li, Q., Evans, G., Glenney M. and Pareek, V., 2010. "Hydrodynamic Simulation of Cyclone Separators", Computational Fluid Dynamics.